JACC: BASIC TO TRANSLATIONAL SCIENCE VOL. 8, NO. 5, 2023

ORIGINAL RESEARCH - PRECLINICAL

Macrophage-Specific NLRC5 Protects From Cardiac Remodeling Through Interaction With HSPA8

Qing Yu, MD,[a,*] Peinan Ju, PhD,[a,*] Wenxin Kou, PhD,[a] Ming Zhai, PhD,[a] Yanxi Zeng, MD,[a] Nuerbiyemu Maimaitiaili, MD,[a] Yefei Shi, PhD,[a] Xu Xu, PhD,[a] Yifan Zhao, PhD,[a] Weixia Jian, PhD,[b] Mark W. Feinberg, PhD,[c] Yawei Xu, PhD,[a] Jianhui Zhuang, PhD,[a] Wenhui Peng, PhD[a]

VISUAL ABSTRACT

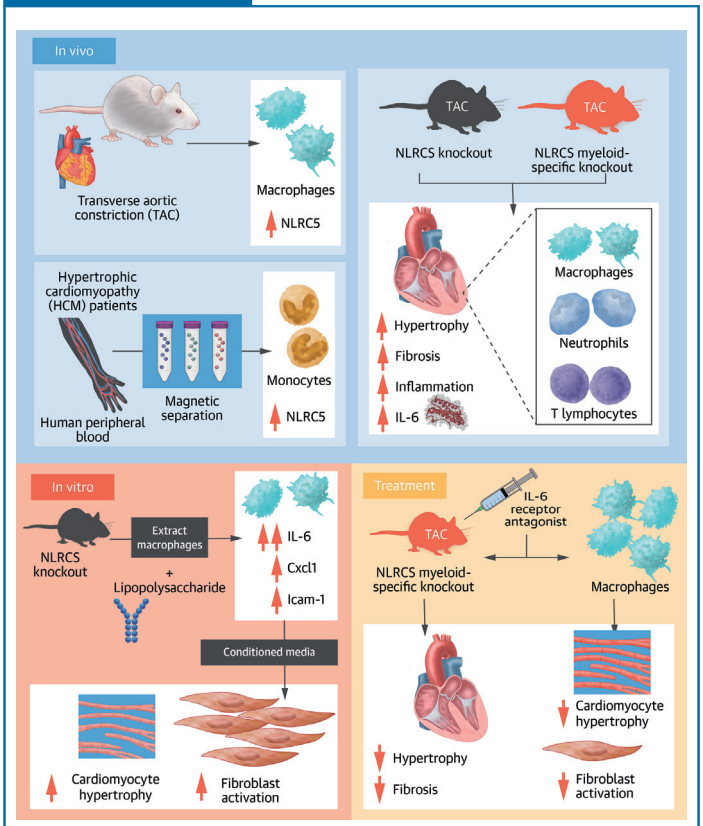

Yu Q, et al. J Am Coll Cardiol Basic Trans Science. 2023;8(5):479-496.

HIGHLIGHTS

- **Macrophages regulate inflammation and the process of tissue repair. Persistent immune activation and inflammation also play a vital role in HF.**
- **In patients with hypertrophic cardiomyopathy, NLRC5 was significantly increased in circulating monocytes and cardiac macrophages. Macrophage-specific NLRC5 protects from adverse remodeling by attenuating inflammation.**
- **Mechanistically, NLRC5 interacted with HSPA8 and suppressed the NF-κB pathway in macrophages. The absence of NLRC5 in macrophages promoted the secretion of cytokines IL-6, which affected cardiomyocyte hypertrophy and cardiac fibroblast activation.**
- **Tocilizumab, an anti-IL-6 receptor antagonist, may be a novel therapeutic strategy for cardiac remodeling and chronic HF.**

From the [a]Department of Cardiology, Shanghai Tenth People's Hospital, School of Medicine, Tongji University, Shanghai, China; [b]Department of Endocrinology, Xinhua Hospital, Shanghai Jiaotong University, School of Medicine, Shanghai, China; and the [c]Cardiovascular Division, Department of Medicine, Brigham and Women's Hospital, Harvard Medical School, Boston, Massachusetts, USA. *Drs Yu and Ju contributed equally to this work.

ISSN 2452-302X https://doi.org/10.1016/j.jacbts.2022.10.001

JACC: BASIC TO TRANSLATIONAL SCIENCE VOL. 8, NO. 5, 2023
MAY 2023:479–496

ABBREVIATIONS AND ACRONYMS

BM = bone marrow

BMDM = bone marrow–derived macrophages

CF = cardiac fibroblast

CM = cardiomyocyte

DEG = differentially expressed gene

EF = ejection fraction

FS = fractional shortening

GO = gene ontology

HCM = hypertrophic cardiomyopathy

HF = heart failure

HSPA8 = heat shock protein 8

HW = heart weight

IL = interleukin

KO = knockout

LPS = lipopolysaccharide

LV = left ventricle

MACS = magnetic-activated cell sorting

MI = myocardial infarction

MS = mass spectrometry

NLR = NOD-like receptor

NLRC5 = NOD-like receptor family caspase recruitment domain family domain containing 5

TAC = transverse aortic constriction

TL = tibia length

WT = wild-type

SUMMARY

Macrophages regulate inflammation and the process of tissue repair. Therefore, a better understanding of macrophages in the pathogenesis of heart failure is needed. In patients with hypertrophic cardiomyopathy, NLRC5 was significantly increased in circulating monocytes and cardiac macrophages. Myeloid-specific deletion of NLRC5 aggravated pressure overload–induced pathological cardiac remodeling and inflammation. Mechanistically, NLRC5 interacted with HSPA8 and suppressed NF-κB pathway in macrophages. The absence of NLRC5 in macrophages promoted the secretion of cytokines such as interleukin-6 (IL-6), which affected cardiomyocyte hypertrophy and cardiac fibroblast activation. Tocilizumab, an anti–IL-6 receptor antagonist, may be a novel therapeutic strategy for cardiac remodeling and chronic heart failure.

Although the incidence of heart failure (HF) has decreased in developed countries with the improvement of cardiovascular disease management, HF. is still a growing health and economic burden, mainly because of the aging population.[1] Besides cardiac remodeling and fibrosis, there are complex pathophysiological processes involved in the development of HF, such as activation of the immune inflammatory response, multiorgan metabolic disorders, and microcirculation dysfunction.[2] Recent studies have directly focused on the effects of proinflammatory cytokines secreted in part by macrophages, leading to the launch of CANTOS (Cardiovascular Risk Reduction Study [Reduction in Recurrent Major CV Disease Events]) using interleukin (IL)-1β antibodies (canakinumab) and RESCUE (Trial to Evaluate Reduction in Inflammation in Patients With Advanced Chronic Renal Disease Utilizing Antibody Mediated IL-6 Inhibition) using IL-6 inhibition (ziltivekimab) for atheroprotection. Accordingly, inhibition of IL-6 receptor by tocilizumab attenuated the inflammatory response and troponin-T release in patients with non-ST-segment elevation myocardial infarction (MI).[3,4] The present evidence shows that macrophages are activated during the early stages of MI/reperfusion injury and cardiac hypertrophy, and contribute to the progression of HF.[5] According to the expression of chemokine receptor type 2 (CCR2) and Timd4, cardiac macrophages can be divided into resident macrophages ($CCR2^{-}Timd4^{+}$) derived from embryonic yolk sac or macrophages differentiated from monocytes ($CCR2^{+}Timd4^{-}$).[6] The early (3 to 7 days) expansion of monocyte-derived cardiac macrophages is required for the excessive inflammatory response, cardiac T-cell expansion, and the transition to HF following pressure overload.[7] Although emerging evidence indicates that $CCR2^{+}Timd4^{-}$ cardiac macrophages are involved in repairing early post-MI injury, the role and mechanism of cardiac macrophages in chronic HF remain unclear.[7,8]

NOD-like receptor family caspase recruitment domain family domain containing 5 (NLRC5) is a member of the NOD-like receptors (NLRs) family belonging to intracellular pattern recognition receptors.[9] It is widely accepted that NLRC5 plays a regulatory role in immune signaling and is highly expressed in immune cells in the spleen, lymph nodes, and bone marrow (BM).[10,11] Our research group conducted a series of studies on NLRC5 protein and demonstrated the protective function of NLRC5 in intimal hyperplasia and angiogenesis.[12,13] On the other hand, Zhou et al[14] reported that NLRC5 deficiency protected heart remodeling by attenuating cardiac fibrosis, but others found that depletion of NLRC5 promoted myocardial injury.[15] Therefore, the exact function of NLRC5 in pressure overload-induced HF remains inconsistent.

Here, we show that *NLRC5* is significantly increased in circulating monocytes and cardiac macrophages from both patients with hypertrophic cardiomyopathy (HCM) and mice with pressure overload. Both global and myeloid-specific deletion of NLRC5 aggravated pressure overload–induced

The authors attest they are in compliance with human studies committees and animal welfare regulations of the authors' institutions and Food and Drug Administration guidelines, including patient consent where appropriate. For more information, visit the Author Center.

Manuscript received August 4, 2022; revised manuscript received October 4, 2022, accepted October 5, 2022.

pathological cardiac remodeling and inflammation. Mechanically, we identified that NLRC5 interacted with heat shock protein 8 (HSPA8) and suppressed NF-κB pathway in macrophages. Depletion of NLRC5 in macrophages promoted IL-6 secretion, which in turn contributed to hypertrophy of cardiomyocytes (CMs) and activation of cardiac fibroblasts (CFs). Conversely, treatment with anti-IL-6 receptor antagonist tocilizumab markedly rescued cardiac remodeling in NLRC5-null mice, indicating a promising therapeutic approach for the treatment of HF.

METHODS

Please see the Supplemental Appendix for detailed methods.

PATIENTS AND CLINICAL SPECIMENS. All experimental procedures were done in accordance with the ethical standards of the responsible institution and follow the guidelines of the Declaration of Helsinki. Written informed consent was obtained from all patients involved in the study according to the local Ethical Committee of Shanghai Tenth People's Hospital (SHSY-IEC-4.1/21-205/01). Fifteen patients were recruited at the Department of Cardiology, and 15 healthy individuals were recruited at the physical examination center from December 2018 to March 2019. For each volunteer, $CD14^+$ monocytes, $CD16^+$ neutrophils, $CD3^+$ T lymphocytes, and $CD19^+$ B lymphocytes were isolated from peripheral blood cells using a magnetic-activated cell sorting (MACS) system. All patients underwent laboratory examination and echocardiography (Supplemental Table 1).

ANIMALS. All experimental procedures involving animals were performed in accordance with the guidelines of the National Institutes of Health (NIH) for the care and use of laboratory animals (NIH Publication, 8th Edition, 2011). Animal studies were approved by the Animal Care and Use Committees of Shanghai Tenth People's Hospital. Global Nlrc5 knockout (KO) mice on C57BL/6J background were obtained from Shanghai Model Organisms Centre and bred as previously described.[12] *Nlrc5*$^{flox/flox}$ mice were generated as described previously.[13] *Nlrc5*$^{flox/flox}$ mice were then crossed with *LysM-Cre* mice (Shanghai Model Organisms Centre) to generate *LysM-Cre/Nlrc5*$^{flox/flox}$ mice. *Nlrc5*$^{+/+}$ (wild-type [WT]) and *Nlrc5*$^{flox/flox}$ (*Nlrc5*$^{fl/fl}$) mice were used as control subjects. Global *Stat1* KO mice on C57BL/6J background were obtained from Shanghai Model Organisms Centre. Transverse aortic constriction (TAC) was applied to induce pressure overload-induced cardiac remodeling in 6-week-old male mice. Four weeks after the operation, all mice were anesthetized via intraperitoneal injections of a xylazine (5 mg/kg) and ketamine (80 mg/kg) mixture, and sacrificed subsequently. Tissue samples were obtained and frozen in liquid nitrogen, then stored at −80°C.

FLOW CYTOMETRY. Peripheral blood cells from each mouse were obtained using heparin anticoagulant tubes. Hearts were then perfused with ice-cold phosphate-buffered saline thoroughly and chopped finely and digested. Red blood cells were lysed for 5 minutes at room temperature. The cell suspensions were then blocked with 0.05 mg/mL anti-mouse CD16/CD32 for 15 minutes at 4°C and then stained with corresponding fluorescently labeled antibodies, diluted in 0.1% bovine serum albumin solution at the indicated concentration (Supplemental Table 2).

CELL CULTURE. Mice were euthanized by CO_2 asphyxiation, and BM was isolated to generate BM-derived macrophages (BMDMs). Macrophage colony-stimulation factor was used for BMDM differentiation.

Neonatal rat CMs and CFs were isolated from 0- to 3-day-old Sprague Dawley rats. Details of isolation protocols are provided in the Supplemental Appendix.

FLUORESCENCE-ACTIVATED CELL SORTING AND MACS. Fluorescence-activated cell sorting was conducted using a BD FACS Aria II (BD Biosciences). MACS with MicroBeads was performed using MS MACS columns and a MACS Separator (Miltenyi Biotec).

MASS SPECTROMETRY. Protein was extracted from BMDMs transfected with adenovirus (Ad)-Control or Ad-Flag-NLRC5. Liquid chromatography-tandem MS/MS analysis was performed on an EASY-nLC 1200 ultrahigh-pressure system combined with Q Exactive Plus high-resolution mass spectrometer via a nano-electrospray ion source (all from Thermo Fisher Scientific) at Shanghai OE Biotech Co., Ltd.

RNA SEQUENCING. BMDMs were transfected with Ad-Control and Ad-Flag-NLRC5 for 24 hours. For BMDMs transfected with Ad-Flag-NLRC5, the duplex small interfering RNA targeting HSPA8 (siHSPA8) and scramble small interfering RNA were then used to stimulate BMDMs for another 24 hours. RNA sequencing was conducted with the help of OE Biotech Co., Ltd.

RNA EXTRACTION AND QUANTITATIVE REAL-TIME POLYMERASE CHAIN REACTION. The total RNA was extracted using Trizol reagent. The complementary DNA was generated from total RNA, and real-time

JACC: BASIC TO TRANSLATIONAL SCIENCE VOL. 8, NO. 5, 2023
MAY 2023:479–496

polymerase chain reaction was performed with specific murine primers. The primer sequences are listed in Supplemental Table 3.

PROTEIN EXTRACTION AND WESTERN BLOT. Expression of proteins was detected using specific antibodies targeted to NLRC5, ANP, HSPA8, IKKβ, p-IKKβ, p38, p-p38, STAT3, p-STAT3, pro-IL-1β, IL-1β, pro-caspase-1, caspase-1, GAPDH, Flag, and Myc. Primary antibodies were then incubated with secondary antibodies for 1 hour, and bends were visualized using chemiluminescence.

STATISTICAL ANALYSIS. Continuous variables are presented as the mean ± SD for at least 3 independent experiments. Results were analyzed using SPSS 14.0 (IBM) and Prism 7.0 (GraphPad Software) software. For continuous data in our experiments, we first calculated the Gaussian distribution of the data using the Kolmogorov-Smirnov test. When 2 groups were compared, *t*-test (Gaussian distribution) or Mann-Whitney test (non-Gaussian distribution) was used. When several groups were compared, statistical significance was determined by analysis of variance with Tukey's post hoc test for multiple pairwise comparisons (Gaussian distribution) or Kruskal-Wallis followed by Dunn's multiple comparison test (non-Gaussian distribution). Statistical analyses of the same individual at different time points were tested using repeated measures analysis of variance (**Figures 1L and 1M**). Differences were considered statistically significant if $P < 0.05$.

RESULTS

NLRC5 EXPRESSION WAS INCREASED IN CARDIAC MACROPHAGES FROM PATIENTS WITH HYPERTROPHIC CARDIOMYOPATHY AND PRESSURE OVERLOAD–INDUCED HF IN MICE. We first screened for the NLR family members in $CD14^+$ monocytes from peripheral blood of patients with HCM and health control subjects by MACS. Although *NLRC5* expression was significantly increased in $CD14^+$ monocytes from HCM patients, the characteristics of other NLR family members remained unchanged except for the down-regulation of *NLRC2* and *NLRC4* in HCM patients (Supplemental Figure 1A). Because human $CD14^+$ monocytes are divided into classical, intermediate, and nonclassical subsets, we further compared the expression of *NLRC5* among these 3 groups of monocytes but did not find significant difference (Supplemental Figures 1B and 1C). We also compared the expression of *NLRC5* in different types of leukocytes from control and HCM patients. The efficiencies of separations of monocytes and neutrophils by MACS were further confirmed by flow cytometry (Supplemental Figure 1D). As shown in **Figure 1A**, the mRNA expression of *NLRC5* was up-regulated in $CD14^+$ monocytes from HCM patients ($P = 0.002$). By contrast, no significant difference in *NLRC5* expression was observed in T lymphocytes, B lymphocytes, and neutrophils (**Figures 1B to 1D**). We then applied immunofluorescent staining to confirm the pathologic changes of NLRC5 in cardiac macrophages between control and HCM patients, and found that NLRC5 expression in cardiac macrophages, but not in CMs, was markedly increased in HCM patients as compared with healthy control subjects (**Figures 1E and 1F**). Appropriate positive and negative control tissues were used to verify the specificity of NLRC5 and CD68 (Supplemental Figures 2A and 2B).

We further evaluated NLRC5 expression in mice subjected to TAC for 1 week or 4 weeks and found that the mRNA and protein levels of NLRC5 were significantly elevated in hearts from TAC-treated mice compared with those from the sham group (**Figures 1G and 1H**). Concordantly, NLRC5 was abundant and markedly increased in cardiac macrophages from TAC-treated mice relative to the sham group (**Figures 1I and 1J**). Corresponding positive and negative control conditions for NLRC5 and CD68 were also conducted in mice (Supplemental Figures 2A and 2B). In addition, we observed NLRC5 rarely colocated with neutrophils and, to some extent, colocalization with T lymphocytes in hearts after 1 week of TAC (Supplemental Figure 2C). In vitro, *Nlrc5* was predominantly expressed in cultured macrophages, including peritoneal macrophages and BMDMs (Supplemental Figure 3A). *Nlrc5* mRNA levels were significantly up-regulated in isolated cardiac macrophages from mouse failing hearts compared with the sham group (**Figure 1K**). Similarly, *Nlrc5* was increased in murine BMDMs stimulated with lipopolysaccharide (LPS) and angiotensin II (Ang II) (**Figures 1L and 1M**). The protein level of NLRC5 was increased in BMDM after LPS stimulation, consistent with the trend of mRNA expression (Supplemental Figure 3B). To further investigate the upstream pathway regulating NLRC5 expression, we isolated BMDMs from $Stat1^{-/-}$ mice and found that LPS stimulation failed to activate NLRC5, indicating that the STAT1-dependent pathway regulates NLRC5 expression (Supplemental Figure 3C). These results suggest that elevated NLRC5 in cardiac macrophages may be associated with pathologic cardiac remodeling.

FIGURE 1 **NLRC5 Expression Was Increased in Monocytes and Cardiac Macrophages From HCM Patients and TAC-Operated Mice**

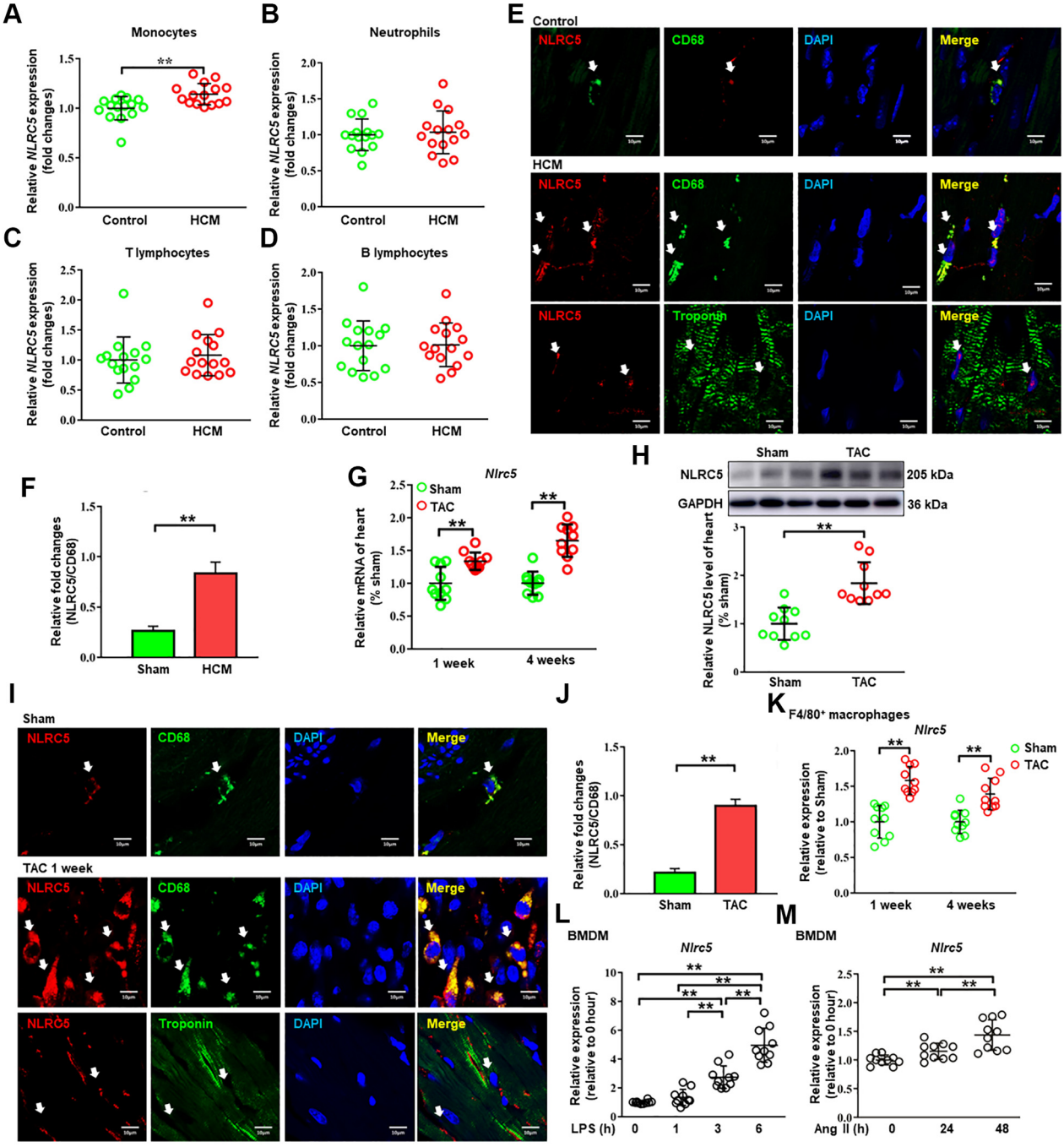

Continued on the next page

JACC: BASIC TO TRANSLATIONAL SCIENCE VOL. 8, NO. 5, 2023
MAY 2023:479–496

GENETIC DELETION OF NLRC5 PROMOTED CARDIAC REMODELING, FIBROSIS, AND HEART FAILURE INDUCED BY PRESSURE OVERLOAD IN MICE. Next, we attempted to determine the role of NLRC5 in pathologic cardiac remodeling and HF through global KO of NLRC5 in mice. There was no difference in body weight, blood pressure, and heart rate between WT and KO mice whether receiving TAC operation or not (Supplemental Figures 4A to 4D). As compared with WT mice, we observed larger heart sizes in KO mice after TAC surgery by gross morphology (**Figure 2A**). The ratio of heart weight to tibia length (HW/TL) was higher in KO mice in response to TAC compared with WT mice (**Figure 2B**). We then measured the cross-sectional areas of CMs in each group by hematoxylin and eosin and wheat germ agglutinin staining, finding an increased cross-sectional area in KO mice than that in WT mice after TAC surgery (**Figures 2C and 2D**). Moreover, successful deletion of *Nlrc5* gene (**Figure 2E**) substantially up-regulated the mRNA and protein expression of the hypertrophy-related markers, such as atrial natriuretic peptide (*Anp*) and brain natriuretic peptide (*Bnp*) after TAC surgery (**Figures 2F and 2G**). Echocardiography was performed to evaluate the cardiac structure and functional changes (**Figure 2H**). After TAC surgery, KO mice exhibited a reduction of ejection fraction (EF) and fractional shortening (FS) compared with WT mice (**Figures 2I and 2J**), along with equivalence of the TAC gradients between groups (Supplemental Figure 4E). TAC-operated KO mice developed enhanced cardiac hypertrophy documented as increased left ventricular (LV) internal diameter, LV posterior wall diameter, and LV mass compared with WT mice (**Figures 2K to 2M**). The collagen volume assessed by Masson staining was remarkably higher in KO hearts than in WT hearts (**Figure 2N**). Consistently, the mRNA expression and immunostaining of fibrotic markers fibronectin and collagen I were significantly increased in KO mice compared with WT mice (**Figures 2O to 2Q**). Similarly, NLRC5 deletion accelerated cardiac remodeling in female mice (Supplemental Figure 5). These data suggest that NLRC5 deficiency aggravates pressure overload-induced cardiac hypertrophy and fibrosis.

NLRC5 DEFICIENCY PROMOTED LEUKOCYTE INFILTRATION IN MOUSE FAILING HEARTS. To investigate whether NLRC5 deficiency influenced TAC-induced macrophage infiltration, we evaluated $CD45^+CD11b^+F4/80^+MerTK^+CD64^+$ macrophages by flow cytometry (Supplemental Figure 6). At 1 week post-TAC, there was a significant increase in total $F4/80^+MerTK^+CD64^+$ macrophages in KO hearts compared with WT hearts, whereas the number of $F4/80^+MerTK^+CD64^+$ macrophages was not changed between the 2 groups after sham operation (**Figures 3A and 3B**). When examining resident and infiltrating subsets, we found that the number of $CCR2^-Timd4^+$ resident macrophages was not significantly changed (Supplemental Figure 7). However, $CCR2^+Timd4^-$ infiltrating macrophages were markedly elevated in KO hearts compared with WT hearts after 1 week of TAC operation (**Figures 3C and 3D**). Although $Ly6G^+$ neutrophils accumulated more in KO hearts vs WT hearts (**Figures 3E and 3F**), the numbers of circulating $Ly6G^+$ neutrophils decreased in peripheral blood (**Figure 3G**). Circulating $Ly6C^+$ monocytes were elevated in KO mice vs WT mice (**Figure 3H**).

It is reported that $CD4^+$ and $CD8^+$ T cells gradually infiltrated the heart and peaked on day 28 after TAC

FIGURE 1 Continued

(A to D) The mRNA expression of *NLRC5* was analyzed in monocytes **(A)**, neutrophils **(B)**, T lymphocytes **(C)**, and B lymphocytes **(D)** isolated from the peripheral blood of healthy control subjects and hypertrophic cardiomyopathy (HCM) patients (n = 15 per group). **(E)** Representative immunofluorescence staining showed that NLRC5 **(red)** was up-regulated in $CD68^+$ macrophages **(green)** in HCM patients as compared with control subjects, but NLRC5 was rarely located in cardiomyocytes (labeled with troponin T in **green**). Scale bars, 10 μm. **(F)** Quantitative analysis of the percentages of NLRC5 in CD68-stained macrophages in HCM patients compared with control subjects (n = 3 per group). Five fields per section from each sample were analyzed. **(G)** The mRNA levels of *Nlrc5* in hearts were detected after 1 and 4 weeks of transverse aortic constriction (TAC) surgery (n = 10 per group). **(H)** Western blots and quantitative analyses were performed to determine the protein expression of NLRC5 in hearts of sham and TAC-treated mice for 4 weeks (n = 10 per group). **(I)** Representative immunofluorescence staining showed that NLRC5 **(red)** was constitutively colocalized with macrophages (labeled with CD68 in **green**) in hearts after 1 week of TAC operation and was rarely expressed in cardiomyocytes. Scale bars, 10 μm. **(J)** Quantitative analysis of the percentages of NLRC5 in CD68-stained macrophages in sham and TAC heart from C57BL/6 mice after 1-week TAC operation (n = 5 per group). Five fields per section from each sample were analyzed. **(K)** The mRNA expression of *Nlrc5* was analyzed in $F4/80^+$ macrophages isolated from hearts after 1 or 4 weeks of TAC (n = 10 per group). The control was heart tissue taken from sham mice at either 1 or 4 weeks after surgery. **(L and M)** The mRNA expression of *Nlrc5* was analyzed in bone marrow–derived macrophages (BMDMs) with liposaccharide (LPS) treatment at 0, 1, 3, or 6 hours (**L**) and with angiotensin II (Ang II) treatment at 0, 24, or 48 hours **(M)** (n = 10 per group). Data are expressed as mean ± SD. $^*P < 0.05$, $^{**}P < 0.01$. Data in **L** and **M** were analyzed using repeated measures analysis of variance. Other data were analyzed using Student's unpaired *t*-test.

FIGURE 2 **NLRC5 Deletion Promoted Cardiac Remodeling Induced by Pressure Overload**

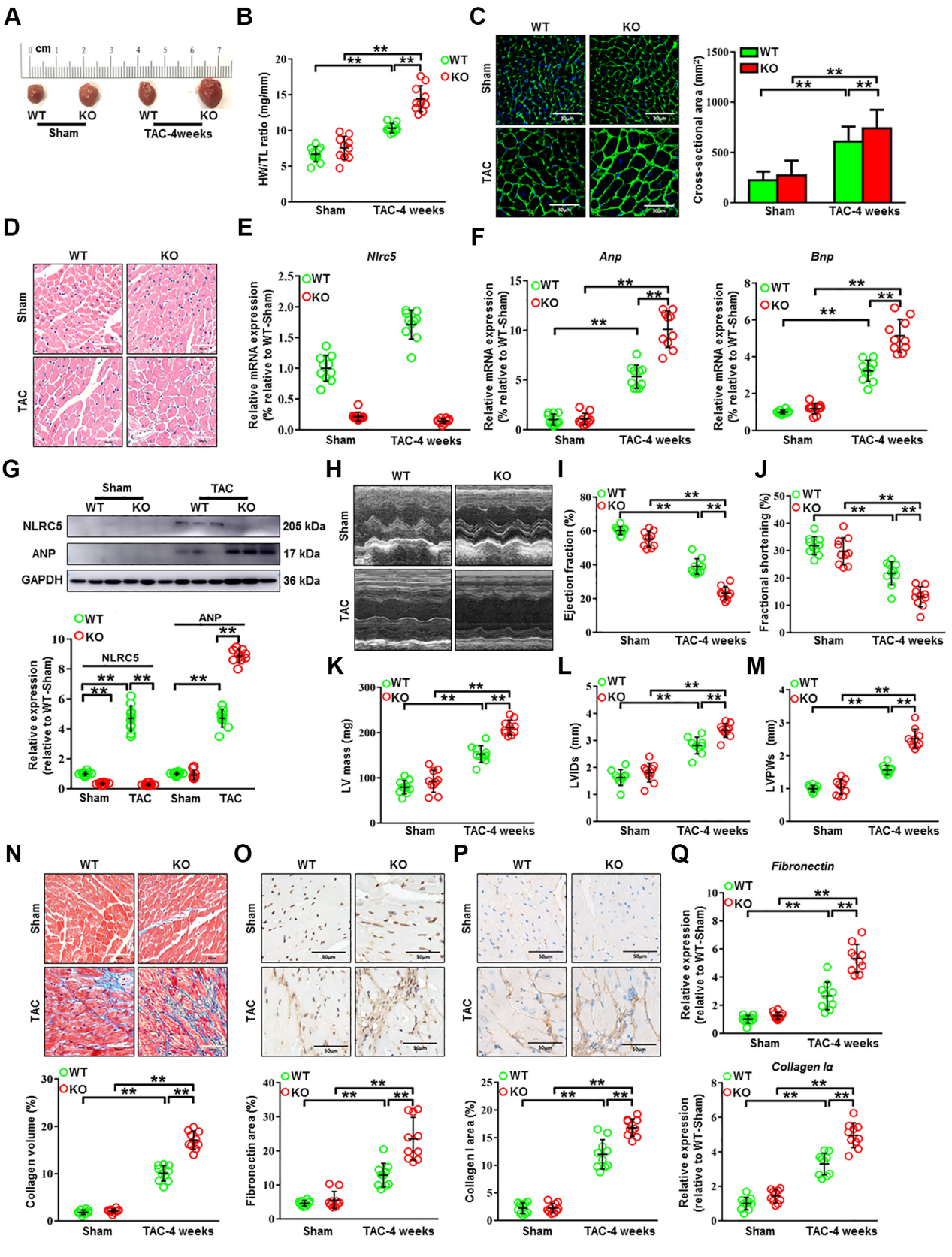

Continued on the next page

JACC: BASIC TO TRANSLATIONAL SCIENCE VOL. 8, NO. 5, 2023
MAY 2023:479–496

operation.[16] In our study, measurement of T lymphocyte abundance at 4 weeks post-TAC indicated that total $CD3^+$ T lymphocytes, $CD4^+$ and $CD8^+$ T subsets were significantly expanded in KO hearts vs WT hearts after TAC surgery (**Figures 3I to 3K**). A similar phenomenon was observed in blood (**Figures 3L to 3N**). These results imply that global absence of NLRC5 enhances circulating monocyte, neutrophil, and lymphocyte infiltration in TAC-induced hearts.

MYELOID-SPECIFIC NLRC5 DELETION AGGRAVATED PRESSURE OVERLOAD–INDUCED HEART FAILURE. To exclude the role of non-BM cells in NLRC5-mediated cardiac remodeling, we performed BM transplantation as previously described.[12] Both WT and KO recipient mice were transplanted with BM from WT donor mice. After 4 weeks of BM transplantation, the chimeric mice were operated with TAC (Supplemental Figure 8A). The cross-sectional areas of CMs, the expression of hypertrophy-related markers, as well as echocardiographic parameters including EF and FS, were comparable between WT and KO recipient mice (Supplemental Figures 8B to 8E). In parallel, the collagen volume and the expression of cardiac fibrosis markers *Fibronectin* and *Collagen Iα* remained unchanged (Supplemental Figures 8F to 8I). The pressure gradients between WT and KO recipient mice groups were comparable 4 weeks after TAC operation (Supplemental Figure 8J). Of note, depletion of NLRC5 in non-BM-derived cells did not alter the number of $F4/80^+MerTK^+CD64^+$ macrophages, $CCR2^+Timd4^-$ subsets, and $Ly6G^+$ neutrophils in hearts after 1 week of TAC (Supplemental Figure 9). Therefore, adoptive transfer of BM-derived macrophages from WT mice to WT and KO mice does not affect HF, suggesting that NLRC5 from non-BM-derived cells does not have a prominent influence on cardiac remodeling.

To validate the contribution of macrophage-derived NLRC5 on HF, $Nlrc5^{flox/flox}$ mice were crossed with *LysM-Cre* mice to generate *LysM-Cre/*$Nlrc5^{flox/flox}$ mice. Littermates not carrying *LysM-Cre* ($Nlrc5^{fl/fl}$) transgene served as control subjects (Supplemental Figure 10). Similar to global KO mice, *LysM-Cre/*$Nlrc5^{flox/flox}$ mice substantially exacerbated cardiac hypertrophy, indicated by increased heart size, HW/TL, the cross-sectional areas of CMs, and the expression of hypertrophy-related markers (**Figures 4A to 4D**). Although the pressure gradients between TAC groups were equivalent (Supplemental Figure 8K), *LysM-Cre/*$Nlrc5^{flox/flox}$ mice also developed a decline in echocardiographic parameters EF and FS, accompanied with enhanced LV mass after 4 weeks of TAC compared with $Nlrc5^{fl/fl}$ mice (**Figures 4E to 4G**). Significant aggravating changes in cardiac fibrosis were reflected by collagen volume and the expression of cardiac fibrosis markers (**Figures 4H to 4J**). Notably, $F4/80^+MerTK^+CD64^+$ macrophages and $CCR2^+Timd4^-$ subsets were remarkably increased in hearts of *LysM-Cre/*$Nlrc5^{flox/flox}$ mice vs $Nlrc5^{fl/fl}$ mice after 1 week of TAC (**Figures 4K to 4M**). By contrast, $CCR2^-Timd4^+$ subsets were not significantly changed (Supplemental Figure 11). Consistently, $Ly6G^+$ neutrophils were increased in the hearts of *LysM-Cre/*$Nlrc5^{flox/flox}$ mice vs $Nlrc5^{fl/fl}$ mice, whereas circulating $Ly6C^+$ monocytes and $Ly6G^+$ neutrophils were comparable between the 2 groups after TAC (**Figures 4N to 4P**). These findings strongly suggest that ablating NLRC5 in myeloid cells promotes cardiac remodeling and macrophage infiltration, predisposing HF.

FIGURE 2 Continued

(A) Gross morphology of hearts from wild-type (WT) and knockout (KO) mice after 4 weeks of transverse aortic constriction (TAC). **(B)** The ratios of heart weight and tibia length (HW/TL) in WT and KO mice (n = 10 per group). **(C)** Histological analysis of cardiomyocyte area was measured by wheat germ agglutinin staining. Scale bars, 30 μm. **(D)** Representative images of transverse area of cardiomyocytes detected by hematoxylin and eosin staining. The cross-sectional areas of cardiomyocytes were analyzed by ImageJ (NIH) (n = 10 per group). Ten fields per section from each sample are analyzed. **(E)** The mRNA expression of *Nlrc5* was assessed in heart tissues, normalized to *Gapdh* (n = 10 per group). **(F)** Relative mRNA expression of cardiac hypertrophy–related markers *Anp* and *Bnp* was assessed (n = 10 per group). **(G)** Representative Western blots determined the protein expression of ANP and NLRC5 in WT and KO mice after 4 weeks of TAC operation (n = 10 per group). **(H to M)** Echocardiographic analyses of ejection fraction, fractional shorting, left ventricular internal diameter at end-systole (LVIDs), left ventricular posterior wall diameter at end-systole (LVPWs), and left ventricular (LV) mass after 4 weeks of TAC operation (n = 10 per group). **(N)** Representative Masson's trichrome staining and quantitative analysis of collagen volume of hearts from WT and KO mice after sham or TAC operation (n = 10 per group). Scale bars, 50 μm. **(O and P)** Immunohistochemistry staining and quantitative analysis of cardiac fibrosis reflected by fibronectin and collagen I in WT and KO mice with sham or TAC operation (n = 10 per group). Scale bars, 50 μm. **(Q)** Relative mRNA expression of cardiac fibrosis markers *Fibronectin* and *Collagen Iα* was measured in heart tissues from WT and KO mice with sham or TAC operation (n = 10 per group). Data are expressed as mean ± SD. $*P < 0.05$, $**P < 0.01$. Data in **E** and **F** were analyzed using Kruskal-Wallis followed by Dunn's multiple comparison test. Other data were analyzed using 1-way analysis of variance followed by Tukey's post hoc analysis.

FIGURE 3 **NLRC5 Deficiency Promoted the Infiltration of Immune Cells After TAC Operation**

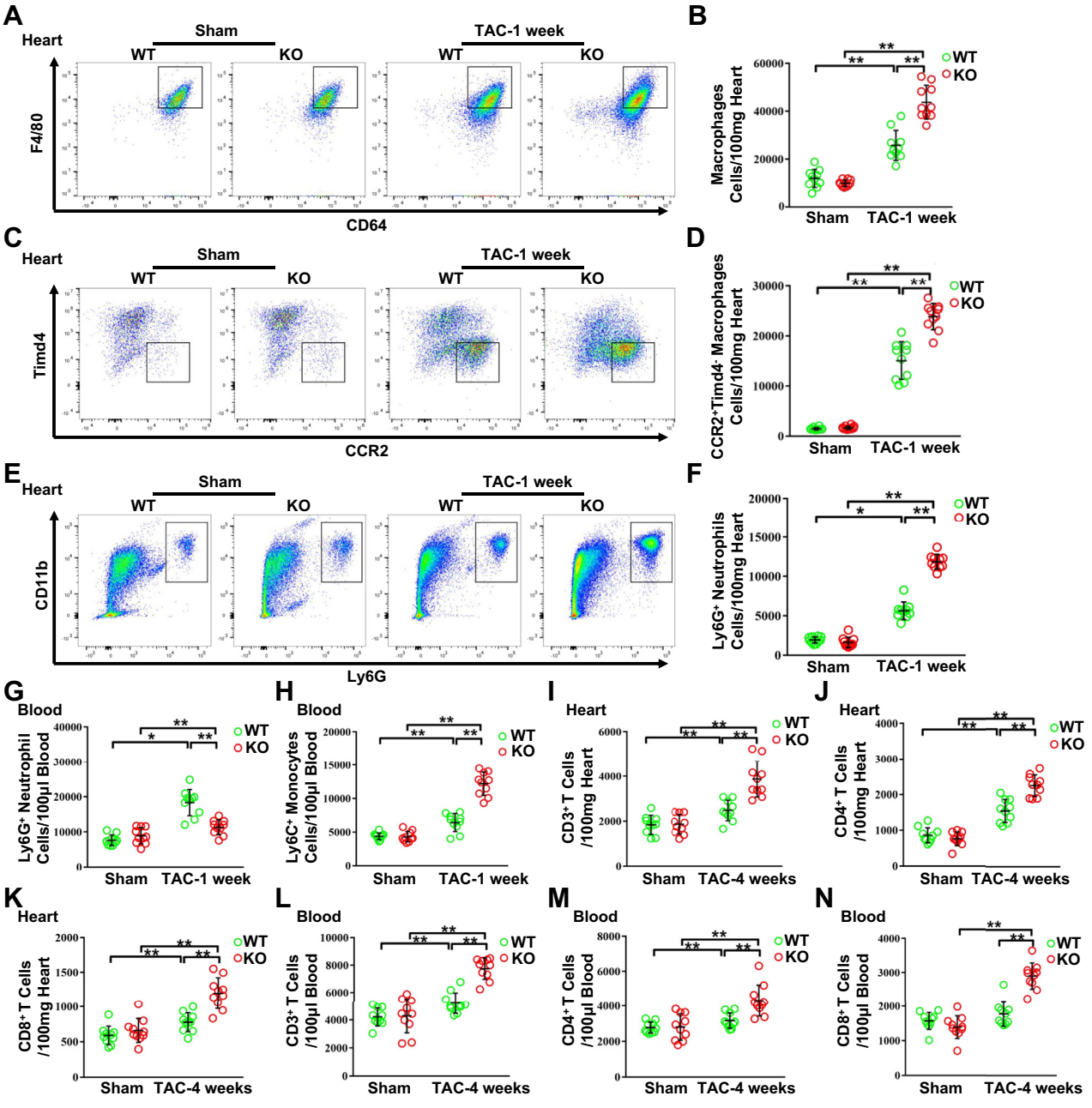

(A and B) Representative cytograms and quantitative analysis of F4/80$^+$ CD64$^+$MerTK$^+$ macrophages in heart tissues (n = 10 per group). **(C and D)** Representative cytograms and quantitative analysis of CCR2$^+$Timd4$^-$ macrophages in heart tissues (n = 10 per group). **(E and F)** Representative cytograms and quantitative analysis of Ly6G$^+$ neutrophils in heart tissues (n = 10 per group). **(G and H)** Quantitative analysis of Ly6G$^+$ neutrophils (**G**) and Ly6C$^+$ monocytes **(H)** in peripheral blood after 1 week of TAC (n = 10 per group). **(I to K)** Quantitative analysis of CD3$^+$ T cells **(I)**, CD4$^+$ T cells **(J)**, and CD8$^+$ T cells **(K)** in heart tissues after 4 weeks of TAC. **(L to N)** Quantitative analysis of CD3$^+$ T cells **(L)**, CD4$^+$ T cells **(M)**, and CD8$^+$ T cells **(N)** in peripheral blood after 4 weeks of TAC (n = 10 per group). Data are expressed as mean ± SD. *P < 0.05, **P < 0.01. Data were analyzed using 1-way analysis of variance followed by Tukey's post hoc analysis. Abbreviations as in Figure 2.

FIGURE 4 Myeloid-Specific NLRC5 Deficiency Exacerbated Cardiac Remodeling Induced by Pressure Overload

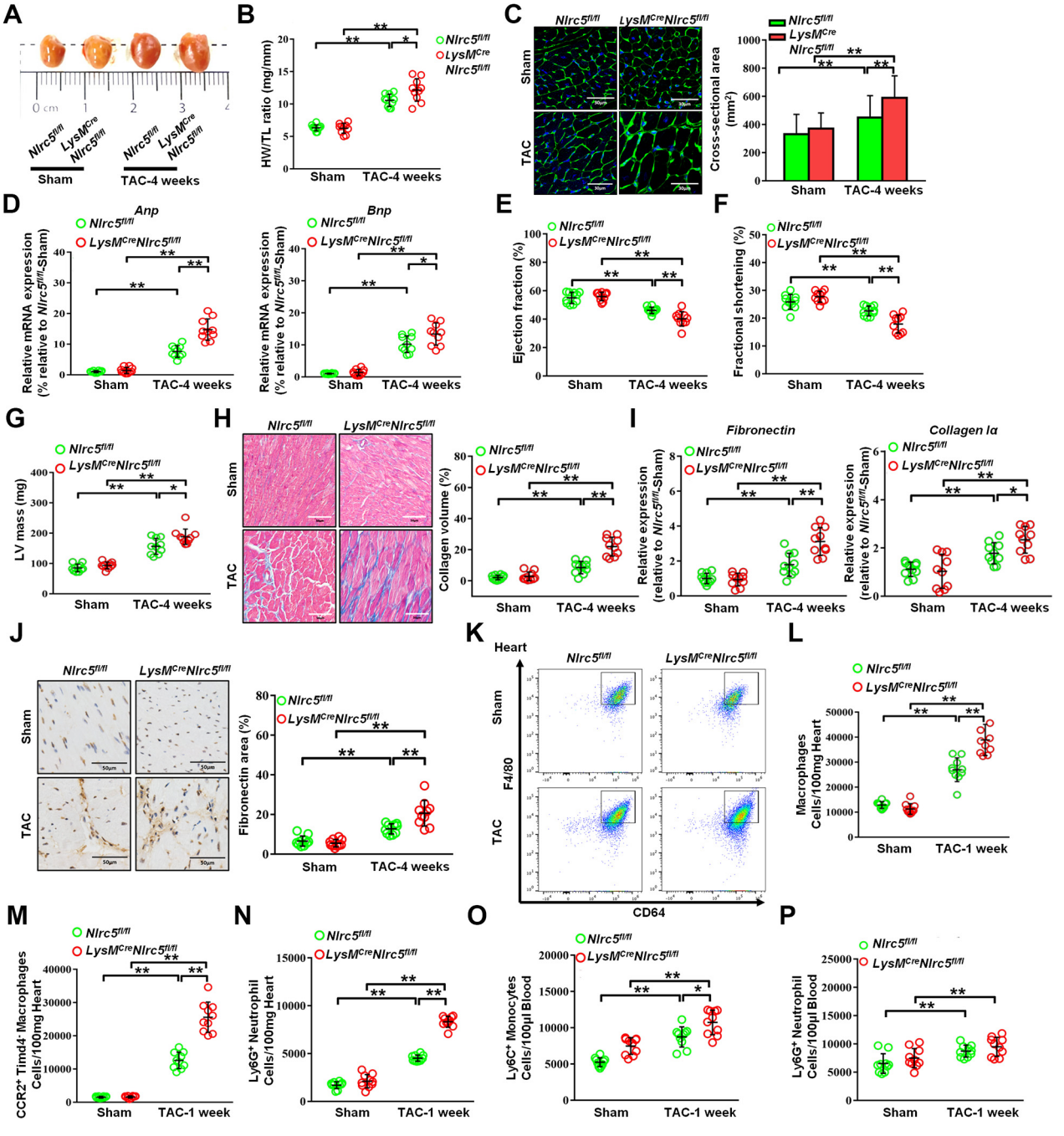

Continued on the next page

NLRC5 INTERACTED WITH HSPA8 IN MACROPHAGES. We first identified the gene expression profile of NLRC5 KO macrophages. The results suggested that the deletion of NLRC5 gene could regulate the expression of immune system process and extracellular matrix-related genes in BMDM and cardiac macrophages (Supplemental Figures 12A and 12B). Therefore, to further investigate the mechanism of NLRC5 in macrophages regulating HF, we performed immunoprecipitation-MS in BMDMs with adenovirus overexpressing NLRC5 in a strategy to capture potential interactors. Through the experimental data and analysis of 3 groups of overexpressed NLRC5, we obtained 6 potential target proteins interacting with NLRC5 (**Figure 5A**). Based on cardiac remodeling related pathway analysis by previous reports,[17,18] HSPA8 was proposed to be a binding protein of NLRC5. The mRNA and protein levels of HSPA8 were consistently increased in the tissues and F4/80$^+$ macrophages of TAC-induced hearts and in LPS-induced BMDMs (**Figures 5B to 5E**). Immunoprecipitation assays revealed an interaction between NLRC5 and HSPA8 in macrophages (**Figure 5F**). Likewise, Flag-tagged NLRC5 successfully coimmunoprecipitated Myc-tagged HSPA8 in HEK293T cells (**Figure 5G**). Confocal microscopy showed that NLRC5 and HSPA8 colocalized in cardiac macrophages after 1 week of TAC surgery (**Figure 5H**) and BMDMs whether treated with LPS or not in vitro (Supplemental Figure 12C).

To further investigate the potential mechanism and regulatory pathways, we performed RNA sequencing of overexpressed NLRC5 and HSPA8 knockdown (siHSPA8) in BMDMs. Gene ontology (GO) analysis showed that NLRC5 overexpression regulated differentially expressed genes (DEGs) involved in several biological processes including regulation of immune response, inflammation, mononuclear cell migration, and IL-6-mediated signaling pathway (**Figure 5I**). Furthermore, GO analysis of DEGs in NLRC5-overexpressing BMDMs with and without siHSPA8 treatment showed that knockdown of HSPA8 participated in regulation of the immune and inflammatory response (**Figure 5K**). We also predicted downstream pathways through gene set variation analysis of DEG enrichment, finding that NLRC5-HSPA8 might play a critical role in regulation of NF-κB signaling and NOD-like receptor pathway (**Figures 5J and 5L**). Because NLRC5 strongly inhibited NF-κB-dependent responses by interacting with IKKβ and blocking its phosphorylation,[19,20] we hypothesized that NLRC5 might suppress NF-κB pathway dependent upon HSPA8. Hence, we first demonstrated that HSPA8 overexpression facilitated the interaction of NLRC5 with IKKβ in the macrophage cell line RAW264.7 (**Figure 5M**). Conversely, knockdown of HSPA8 by siHSPA8 abrogated the interaction of NLRC5 with IKKβ (**Figure 5N**).

MACROPHAGE NLRC5 FACILITATED IL-6 SECRETION TO EXACERBATE CARDIAC REMODELING. On the basis of mouse cytokine array profiling, we found that NLRC5 silencing promoted some cytokine secretion including IL-6, CXCL1, and sICAM-1 in macrophages under LPS stimulation (**Figures 6A and 6B**). Quantitative real-time polymerase chain reaction validated that the expression of *Il-6*, *Cxcl1*, and *Icam-1* was remarkably increased in F4/80$^+$ macrophages isolated from global KO hearts compared with WT hearts (**Figure 6C**). Although *Il-6* expression was prominently higher in KO BMDMs induced by LPS than those in WT BMDMs, the expression of *Cxcl1* and *Icam-1* was moderately up-regulated in KO BMDMs (**Figure 6D**). Enzyme-linked immunosorbent assay revealed that the content of IL-6 in circulating blood of KO mice

FIGURE 4 Continued

(A) Gross morphologies of hearts from *Nlrc5*$^{flox/flox}$ (*Nlrc5*$^{fl/fl}$) and *LysM-Cre/Nlrc5*$^{flox/flox}$ mice after 4 weeks of TAC. **(B)** The ratios of HW/TL in *Nlrc5*$^{fl/fl}$ and *LysM-Cre/Nlrc5*$^{flox/flox}$ mice after TAC (n = 10 per group). **(C)** Representative images of transverse area of cardiomyocytes detected by wheat germ agglutinin staining. Scale bars, 30 μm. The cross-sectional areas of cardiomyocytes were analyzed by ImageJ (NIH) (n = 10 per group). Ten fields per section from each sample were analyzed. **(D)** Relative mRNA expression of cardiac hypertrophy-related markers *Anp* and *Bnp* were assessed (n = 10 per group). **(E to G)** Echocardiography analysis of fractional shorting **(E)**, ejection fraction **(F)**, and LV mass **(G)** after 4 weeks of TAC operation (n = 10 per group). **(H)** Representative Masson's trichrome staining and quantitative analysis of collagen volume of hearts from *Nlrc5*$^{fl/fl}$ and *LysM-Cre/Nlrc5*$^{flox/flox}$ mice after 4 weeks of TAC operation (n = 10 per group). Scale bars, 50 μm. **(I)** Relative mRNA expression of cardiac fibrosis markers *Fibronectin* and *Collagen Iα* were measured in heart tissues from *Nlrc5*$^{fl/fl}$ and *LysM-Cre/Nlrc5*$^{flox/flox}$ mice after 4 weeks of TAC operation (n = 10 per group). **(J)** Immunohistochemistry staining and quantitative analysis of cardiac fibrosis marker fibronectin in *Nlrc5*$^{fl/fl}$ and *LysM-Cre/Nlrc5*$^{flox/flox}$ mice with TAC operation (n = 10 per group). Scale bars, 50 μm. **(K and L)** Representative cytograms of F4/80$^+$ CD64$^+$MerTK$^+$ macrophages in heart tissues **(K)** and quantitative analysis **(L)** (n = 10 per group). **(M and N)** Quantitative analysis of CCR2$^+$Timd4$^-$ macrophages **(M)** and Ly6G$^+$ neutrophils **(N)** in hearts from *Nlrc5*$^{fl/fl}$ and *LysM-Cre/Nlrc5*$^{flox/flox}$ mice after 1 week of TAC operation (n = 10 per group). **(O and P)** Quantitative analysis of Ly6C$^+$ monocytes **(O)** and Ly6G$^+$ neutrophils **(P)** in peripheral blood from *Nlrc5*$^{fl/fl}$ and *LysM-Cre/Nlrc5*$^{flox/flox}$ mice after 1 week of TAC operation (n = 10 per group). Data are expressed as mean ± SD. *$P < 0.05$, **$P < 0.01$. Data were analyzed using 1-way analysis of variance followed by Tukey's post hoc analysis. Abbreviations as in **Figure 2**.

FIGURE 5 NLRC5 Directly Interacted With HSPA8

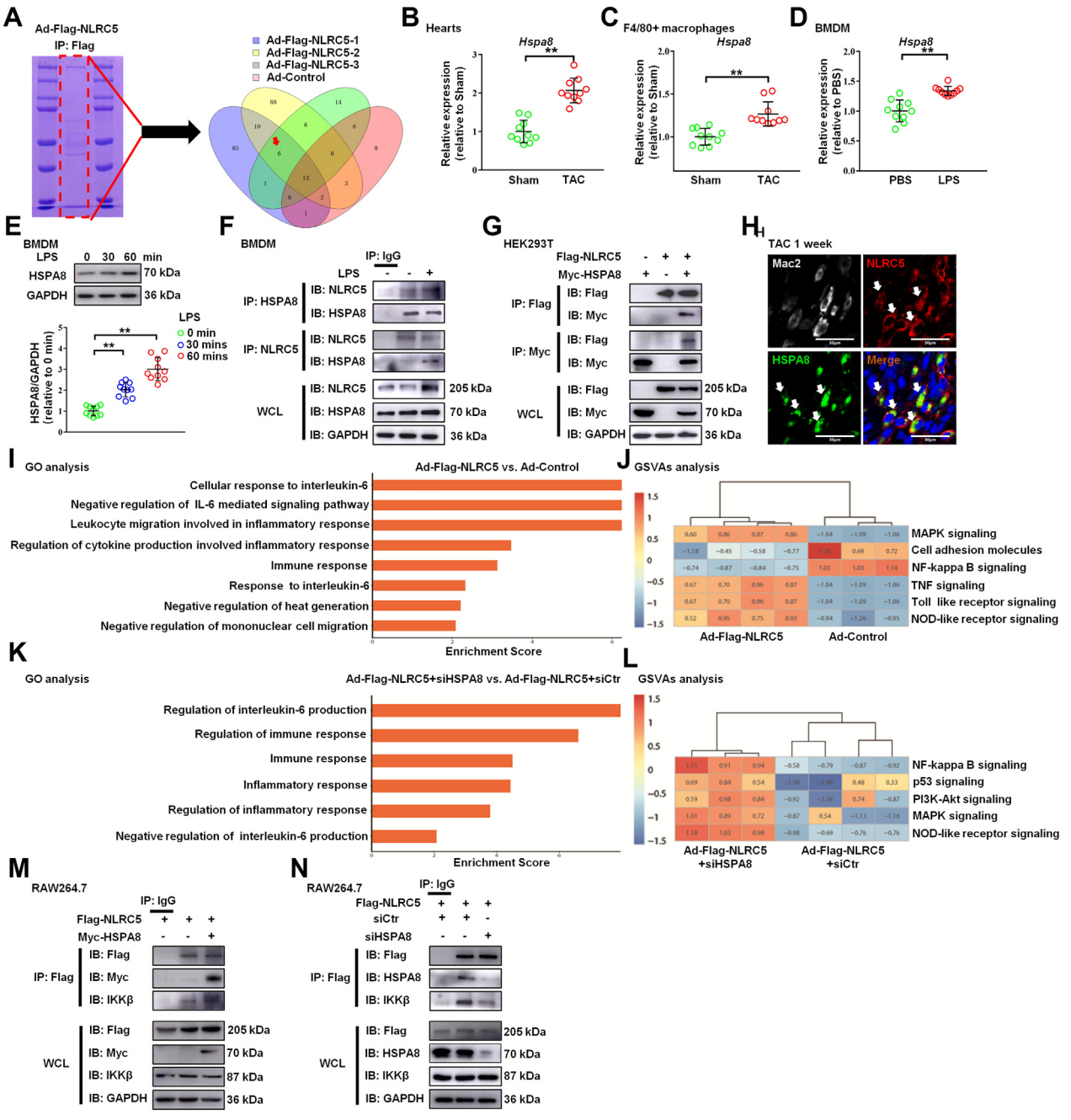

Continued on the next page

after TAC surgery was substantially increased (Supplemental Figure 13A). Meanwhile, as compared with WT mice, the expression of *Il-6* was increased in the liver, kidney, lung, and spleen of KO mice after TAC surgery (Supplemental Figure 13B). Because the regulatory effect of NLRC5 on NLRP3 inflammasome is an ongoing debate,[11,21] it is necessary to explore the effects of NLRC5 deficiency on activation of NLRP3 inflammasome. We found that deletion of NLRC5 has little impact on the generation of caspase-1 and IL-1β in BMDMs under costimulation of LPS and ATP (Supplemental Figure 13C). To address a potential paracrine effect, we cultured neonatal rat CMs and CFs in the presence of conditioned medium from LPS-induced WT and KO BMDMs (**Figure 6E**). Similar to the in vivo findings, CMs cultured in KO BMDM medium displayed severe hypertrophy, indicated by larger CM sizes and higher *Anp* expression (**Figures 6F to 6H**). CFs cultured in KO BMDM medium were also activated, reflected by increased *α-SMA* expression, and converted to a proliferative state indicated by CCK8 assay and EdU staining (**Figures 6I to 6L**). Additionally, STAT3 phosphorylation was enhanced in both CMs and CFs cultured in LPS-induced KO BMDM medium (**Figures 6M and 6N**). These findings suggest that deficiency of NLRC5 in macrophages precipitates the secretion of IL-6 and affects the microenvironment of cardiac remodeling.

NLRC5 DEFICIENCY PROMOTED CARDIAC REMODELING DEPENDENT UPON IL-6 SECRETION FROM MACROPHAGES. We further investigated the potential therapeutic possibility of the IL-6 receptor antagonist tocilizumab in cardiac hypertrophy and dysfunction accelerated by NLRC5 deficiency (Supplemental Figure 14A).[22,23] In order to make the study more valuable for clinical application, we first compared once per 7 days with once per 3 days using the dosage of 5 mg/kg adopted as described in a previous study.[24] Echocardiographic analyses demonstrated that the protective effect of weekly administration of tocilizumab on LV contractility was greater than that of administration of tocilizumab every 72 hours (Supplemental Figures 14B to 14D). Nevertheless, there were no significant changes in HW/TL in TAC-induced mice after different dosages of tocilizumab treatment with a comparable load between TAC groups (Supplemental Figures 14E and 14F). Compared with the control group, tocilizumab (5 mg/kg, per 72 hours, 4 weeks) significantly alleviated TAC-induced cardiac hypertrophy in WT mice, reflected by the attenuation of heart sizes, decreased HW/TL, reduced cross-sectional areas of CMs, and a decline in *Anp* expression (**Figures 7A to 7D**). Strikingly, more apparent improvements in TAC-induced cardiac hypertrophy in NLRC5-deficient mice were observed after 4 weeks of tocilizumab treatment, with equivalence of the TAC gradient between groups (Supplemental Figure 14F). As expected, we observed a significant decrease of Il-6 receptor in TAC-induced failing hearts after tocilizumab treatment (**Figure 7E**). Echocardiographic analyses revealed that Tocilizumab significantly prevented cardiac hypertrophy and dysfunction as reflected by improved EF (27% in TAC vs 39% after TAC with tocilizumab treatment) and FS, and reduced LV mass (**Figures 7F to 7H**). NLRC5-null

FIGURE 5 Continued

(A) The most potential functional binding targets of NLRC5 were evaluated by mass spectrometry of BMDMs with adenovirus (Ad) overexpressing NLRC5. Six potential target proteins were interacting with NLRC5 were screened through 3 batches of overexpressed NLRC5 compared with the result of a control group. **(B)** Relative mRNA expression of *Hspa8* in hearts after TAC. **(C)** Relative mRNA expression of *Hspa8* in F4/80$^+$ macrophages isolated from hearts. **(D)** Relative mRNA expression of *Hspa8* in BMDMs with or without LPS treatment. **(E)** Western blotting and quantitative analysis of HSPA8 and GAPDH in BMDMs from mice with or without LPS treatment. **(F)** Coimmunoprecipitation of NLRC5 and HSPA8 in BMDMs with and without LPS treatment. The lysates immunoprecipitated with anti-IgG serve as a negative control condition. **(G)** HEK293T cells were cotransfected with Flag-tagged NLRC5 and Myc-tagged HSPA8 plasmid. **(H)** Immunofluorescence staining of NLRC5 **(red)**, Mac2 **(grey)**, HSPA8 **(green)**, and nuclei **(blue)** in hearts. Scale bars, 30 μm. **(I)** Gene ontology (GO) enrichment analysis and gene set variation analysis (GSVAs) of the expression of several genes with roles in different biological responses of Ad-Flag-NLRC5 compared with the Ad-negative control (Ad-NC) condition from RNA sequencing. **(J)** GSVAs of the expression of several genes were performed with role in different signaling pathways from RNA sequencing. **(K and L)** GO enrichment analysis and GSVAs analysis of the expression of several genes with role in different biological response and signaling pathways of Ad-Flag-NLRC5 plus siHSPA8 treatment compared with Ad-Flag-NLRC5 from RNA sequencing. **(M)** BMDMs were cotransfected with Flag-tagged NLRC5 and Myc-tagged HSPA8 plasmid. The lysates immunoprecipitated with anti-IgG serve as a negative control condition. **(N)** Coimmunoprecipitation of NLRC5 and IKKβ in BMDMs with or without siHSPA8 treatment. Data are expressed as mean ± SD. *$P < 0.05$, **$P < 0.01$. Data in **B** to **D** were analyzed using Student's unpaired *t*-test. Data in panel **E** were analyzed using 1-way analysis of variance followed by Tukey's post hoc analysis. IB = immunoblotting; IP = immunoprecipitation; WCL = whole cell lysis; other abbreviations as in **Figures 1 and 2**.

FIGURE 6 Deficiency of NLRC5 in Macrophages Facilitated Dysfunction of CMs and CFs Through Promoting the Secretion of IL-6

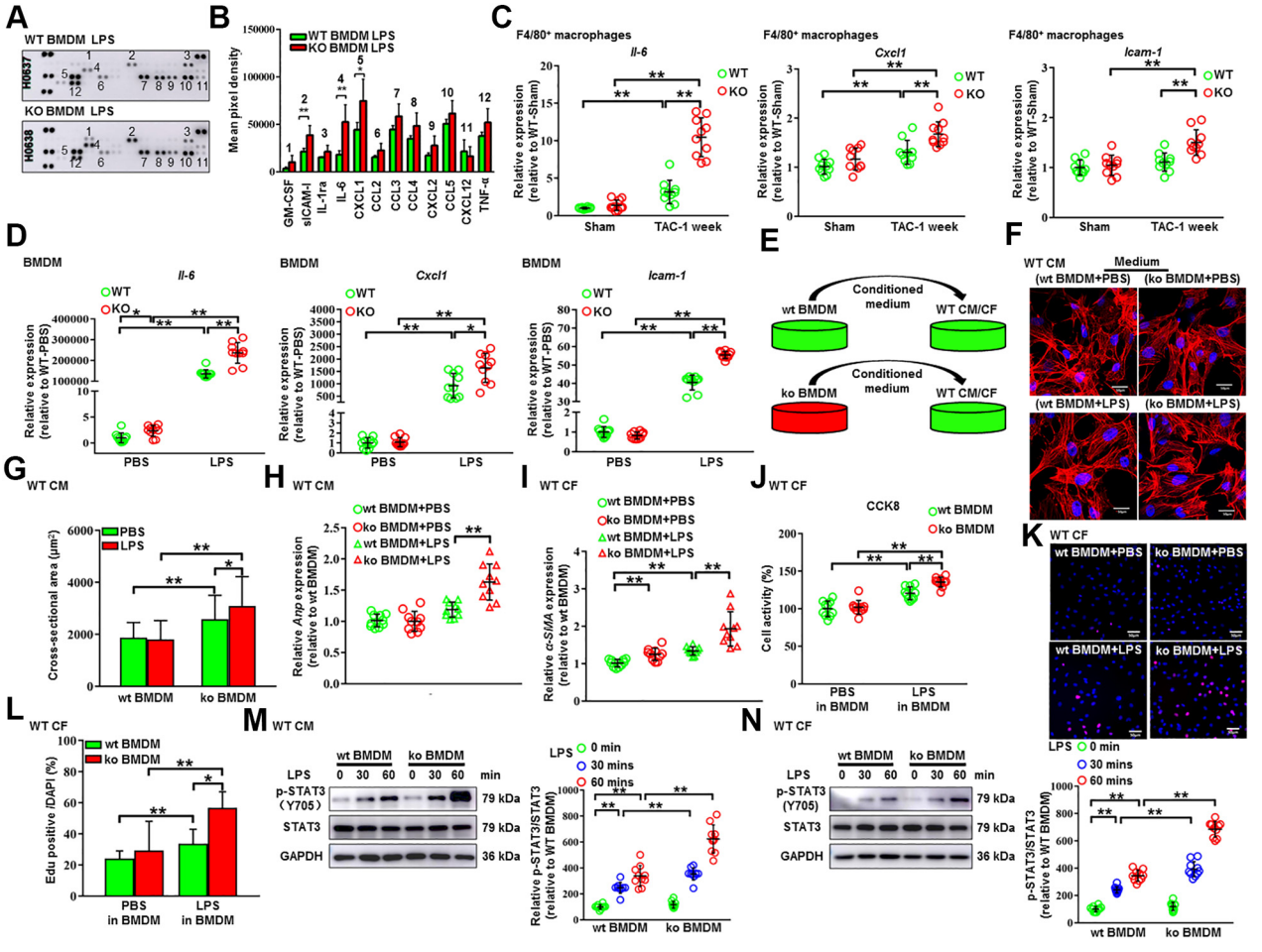

(A and B) The cell culture supernatants of BMDMs from WT and KO mice were detected by mouse cytokine array. BMDMs were treated with 100 ng/mL of LPS for 6 hours, and the relative mean pixel density was calculated (n = 3 per group). **(C)** Relative mRNA expression of proinflammatory cytokines *Il-6*, *Cxcl1*, and *Icam-1* in F4/80$^+$ macrophages isolated from WT and KO hearts was quantified by real-time polymerase chain reaction (n = 10 per group). **(D)** Relative mRNA expression of proinflammatory cytokines *Il-6*, *Cxcl1*, and *Icam-1* in BMDMs from WT and KO mice were quantified by real-time polymerase chain reaction (n = 10 per group). **(E)** Experimental design. Conditional medium was collected from BMDMs of WT (wt BMDM) and KO (ko BMDM) mice in the presence or absence of LPS. The conditional medium was then used to culture WT cardiomyocytes (WT CM). **(F and G)** Representative immunofluorescent images and quantitative analysis of cross-sectional areas of CMs labeled by α-actinin after culturing with conditional medium. More than 100 CMs from each group were randomly selected. Scale bars, 50 μm. **(H)** Relative mRNA expression of *Anp* was quantified by real-time polymerase chain reaction (n = 10 per group). **(I)** Relative mRNA expression of α-*SMA* in CFs cultured with conditional medium from WT and KO BMDMs was quantified by real-time polymerase chain reaction (n = 10 per group). **(J)** The cell activity of cardiac fibroblasts (CFs) was measured by CCK8 kit (n = 10 per group). **(K and L)** The proliferation capacity of CFs was shown in EdU staining (n = 10 per group). Scale bars, 50 μm. **(M)** Representative Western blot and quantitative analysis of p-STAT3 and STAT3 in CMs with conditional medium from WT and KO BMDMs (n = 10 per group). **(N)** Representative Western blot and quantitative analysis of p-STAT3 and STAT3 in CFs with conditional medium from WT and KO BMDMs (n = 10 per group). Data are expressed as mean ± SD. *$P < 0.05$, **$P < 0.01$. Data were analyzed using 1-way analysis of variance followed by Tukey's post hoc analysis. PBS = phosphate-buffered saline; other abbreviations as in Figures 1 and 2.

mice responded to a greater degree than WT mice in preventing TAC-induced cardiac fibrosis, as indicated by *Fibronectin* and *Collagen Iα* expression, after tocilizumab (Figures 7I to 7L). These data indicate that inhibition of IL-6 receptor by tocilizumab could prevent cardiac remodeling and HF, and the more significant benefit of tocilizumab against cardiac remodeling is achieved when NLRC5 is lacking.

FIGURE 7 **IL-6 Receptor Antagonist Tocilizumab Prevented Pathological Cardiac Remodeling Caused by NLRC5 Deficiency**

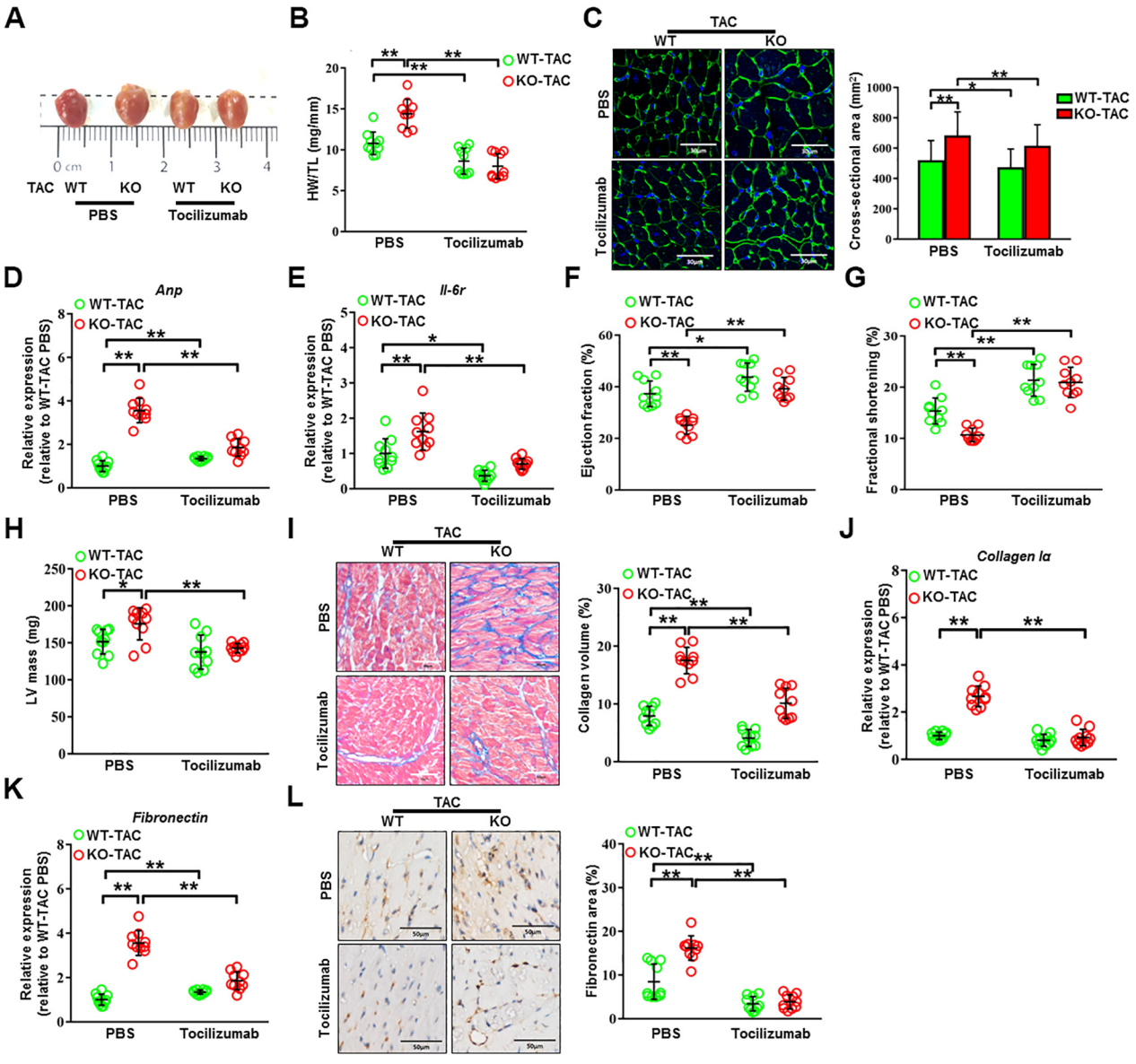

(A) Gross morphologies of hearts from WT and KO mice with and without tocilizumab after TAC surgery. **(B)** HW/TL in WT and KO mice with and without tocilizumab after TAC surgery (n = 10 per group). **(C)** Representative images and quantitative analysis of transverse area of CMs detected by wheat germ agglutinin staining (n = 10 per group). Scale bars, 30 μm. **(D and E)** Relative mRNA expression of *Anp* and *Il-6r* was assessed by real-time polymerase chain reaction (n = 10 per group). **(F to H)** Echocardiography analysis of fractional shorting, ejection fraction, and LV mass after 4 weeks of TAC were shown (n = 10 per group). **(I)** Representative Masson's trichrome staining and quantitative analysis of heart sections from WT and KO mice with and without tocilizumab after TAC surgery (n = 10 per group). Scale bars, 50 μm. **(J and K)** Relative mRNA expression of cardiac fibrosis markers *Fibronectin* and *Collagen Iα* were measured by real-time polymerase chain reaction in hearts from WT and KO mice with and without tocilizumab (n = 10 per group). **(L)** Representative immunohistochemistry staining and quantification analysis of fibronectin in hearts from WT and KO mice with and without tocilizumab (n = 10 per group). Scale bars, 50 μm. Data are expressed as mean ± SD. $^{*}P < 0.05$, $^{**}P < 0.01$. Data were analyzed using 1-way analysis of variance followed by Tukey's post hoc analysis. Abbreviations as in Figures 1, 2, and 6.

JACC: BASIC TO TRANSLATIONAL SCIENCE VOL. 8, NO. 5, 2023
MAY 2023:479–496

DISCUSSION

In this work, we propose a previously unrecognized role of macrophage NLRC5 in the microenvironment of cardiac remodeling.

HF is a complex and multifaceted process, characterized by alterations in excitation-contraction coupling, overwhelming neuroendocrine activation, cardiac energetic deficit, oxidative stress, and chronic immunological response.[25,26] Local inflammatory responses are not only a consequence, but also a driver, of HF.[27] It is accepted that activation of pattern recognition receptors, such as the NLR family, by endogenous stimuli initiates the intracellular signaling cascades that orchestrate the transcription and secretion of proinflammatory cytokines.[28] Of the NLR family members, NLRC5 is predominantly increased in macrophages of mouse and human failing hearts. However, HCM and TAC-induced cardiac hypertrophy could not represent all causes of HF. Further research is required to determine the expression of NLRC5 in other heart diseases such as diabetic cardiomyopathy and ischemic heart disease. In addition, LPS up-regulates the specific damage-related molecular patterns (DAMPs) molecule that induces an acute and transient inflammatory response by activating PRRs, such as NLRs family members in chronic HF.[29-31] Although NLRC5 is moderately located in T lymphocytes, NLRC5 does not change significantly in circulating T lymphocytes of HCM patients as compared with healthy individuals. In addition, the absolute number of T lymphocytes was significantly lower than that of macrophages in TAC-induced hearts. Tissue-residing immune cells and macrophages, especially $CCR2^{+}$ subsets, are known to be dominant at the early phase of hypertrophy and accelerate the transition to HF through various mechanisms.[32,33] However, the specific proteins and the exact mechanisms related to macrophages involved in cardiac remodeling were not well recognized. Our data reveal that deficiency of NLRC5 in macrophages leads to cardiac hypertrophy, cardiac fibrosis, and inflammatory cell recruitment. Our prior experimental data illustrated the pleiotropic protection of NLRC5 on cardiovascular diseases.[12,13] However, published studies failed to draw a consistent conclusion about NLRC5 in HF without sufficient evidence.[14,15,34] These conflicting findings could be explained by the fact that failing hearts involve the buildup of parenchymal cells and infiltrating immune cells. Our in vivo and in vitro data showed that NLRC5 was primarily expressed in macrophages, but not in parenchymal cells. Moreover, the in vivo evidence of cell-specific NLRC5 involvement in the pathogenesis of HF was lacking. Toward this end, we conducted BM transplantation in global *Nlrc5* KO mice and generated *LysM-Cre/Nlrc5*$^{flox/flox}$ mice to dissect the specific role of macrophage NLRC5 in cardiac remodeling. These experiments highlight that NLRC5-deficient cardiac remodeling is mediated through macrophages.

More importantly, we identified a key interaction between NLRC5 and HSPA8 in macrophages and TAC-induced failing hearts through immunoprecipitation-MS analysis. Accumulating studies have shown that the compensatory increases in heat shock proteins, also known as chaperones, lead to deterioration of cardiac dysfunction and play an important role in ischemic reperfusion injury, HF, and arrhythmias.[17,18] In addition, recent studies have demonstrated that inhibition of heat shock protein 70 (HSP70) blocks the development of cardiac hypertrophy, and blocking HSP70 activity may provide potential therapeutic benefits for the treatment of HF.[19] It has been reported that the binding of NLRC5 to IKKβ suppressed IKKβ phosphorylation.[20] Interestingly, our study elucidates that HSPA8 is required for the reciprocal action between NLRC5 and IKKβ. In other words, HSPA8 knockdown partially eliminates the interaction of NLRC5 with IKKβ and reduces the activity of NF-κB pathway in macrophages.

Another intriguing observation in our study is that NLRC5 deficiency in macrophages governs the microenvironment of cardiac remodeling by releasing IL-6, CXCL1, and ICAM-1, thereby promoting CM hypertrophy, activating CFs, and inducing neutrophil and lymphocyte infiltration. When macrophages phagocytize necrotic CMs, TGF-β, IL-6, and IL-10 secreted by macrophages stimulate the transformation of fibroblasts into myofibroblasts and promote collagen deposition of extracellular matrix.[35] Other studies also highlighted the crosstalk between macrophages and other resident cells in failing hearts through paracrine mechanisms of proinflammatory cytokines. For example, CXCL1 conferred neutrophil infiltration in heart tissue.[35] ICAM-1 elicited inflammation accompanied by lymphocyte infiltration and expansion.[36] IL-6 provoked hypertrophy of CMs and conversion of CFs to myofibroblasts by activating the STAT3 pathway.[37] Indeed, exploring the changes in the microenvironment can inform a better understanding of the development of HF, paving the way for clinical transformation.

Although current HF treatments are mostly limited to antagonization of neuroendocrine activation, more recent observations suggest that immunoregulatory

targets are likely to provide substantial prognostic benefit.[38] In this respect, our study demonstrates that tocilizumab reverses cardiac hypertrophy and fibrosis in NLRC5-deficient mice without apparent toxicities. Tocilizumab is an IL-6 receptor antagonist approved for the treatment of various rheumatic diseases.[39-41] A recent study indicated that tocilizumab ameliorated myocardial injury and restored cardiac function via suppression of the systematic inflammatory response in patients experiencing out-of-hospital cardiac arrest.[42] Of note, the repertoire of immunological responses differs in acute myocardial injury and chronic cardiac remodeling.[43] Although tocilizumab attenuated the inflammatory response and troponin-T release in patients with non-ST-segment elevation MI, this phase 2 trial had neutral results for the improvement of cardiac function documented by echocardiographic EF and plasma B-type natriuretic peptide.[44] In agreement with these observations, TAC-induced mice had a significant response to tocilizumab treatment when a more obvious therapeutic effect was observed in NLRC5-null mice. Taken together, this finding raises the possibility that activation of NLRC5 and blockade of IL-6 might cooperatively lessen cardiac remodeling and HF.

STUDY LIMITATIONS. First, we have demonstrated that NLRC5 in macrophages significantly ameliorates pressure overload-induced cardiac hypertrophy and fibrosis by down-regulating the secretion of IL-6 through the interaction of HSPA8. However, we did not rule out a potential indirect interaction between NLRC5 and HSPA8. Mutational analysis of the minimal interacting domain will help in clarifying this issue.

In addition, it has not been directly proven that activation of NLRC5 and blockade of IL-6 improve the prognosis of patients with HF. Tocilizumab has already been shown to be safe and effective in patients with MI. Thus, more preclinical and clinical trials should be conducted to investigate the potential therapeutic effects of Tocilizumab in patients with HF.

CONCLUSIONS

In summary, this study highlights that NLRC5 in macrophages positively impacts cardiac remodeling via interaction with HSPA8, thereby providing a strong pre-clinical foundation that the NLRC5-HSPA8-IL-6 signaling axis may serve as a complementary immunomodulatory therapeutic target for HF.

ACKNOWLEDGMENTS The authors thank the patients who participated in this study. The authors thank Dr Wei Wang of Shanghai XinPu BioTechnology Co., Ltd. for her help in flow cytometry experiments and thank Prof Yi Zhang of Shanghai Tenth People's Hospital, School of Medicine, Tongji University, for his help with the experimental samples.

FUNDING SUPPORT AND AUTHOR DISCLOSURES

Funded by National Natural Science Foundation of China grants 81800424, 81900239, 81670746, 91939101, and 82070230, Clinical Research Plan of SHDC No. SHDC2020CR4019, and the Natural Science Foundation of Shanghai No. 20ZR1435300. The authors have reported that they have no relationships relevant to the contents of this paper to disclose.

ADDRESS FOR CORRESPONDENCE: Dr Wenhui Peng OR Dr Jianhui Zhuang, Department of Cardiology, Shanghai Tenth People's Hospital, Tongji University School of Medicine, 301 Middle Yanchang Road, Shanghai 200072, China. E-mail: pwenhui@tongji.edu.cn OR jh_zhuang@tongji.edu.cn.

PERSPECTIVES

COMPETENCY IN MEDICAL KNOWLEDGE: Despite advances in managing HF, the burden of this progressive syndrome continues to increase with increasing morbidity and mortality. Persistent immune activation and inflammation also play a significant role in HF. Recent clinical trials demonstrated the beneficial effects of immunomodulatory therapy (IL-1β antagonist, canakinumab, CANTOS; NCT01327846; IL-6 receptor antagonist, tocilizumab, ASSessing the Effect of Anti-IL-6 Treatment in Myocardial Infarction: The ASSAIL-MI Trial [ASSAIL-MI]; NCT03004703) in MI, but the immunomodulatory protein in pressure overload–induced cardiac remodeling and HF remained poorly understood. To address this knowledge gap, the present study recognized NLRC5 as a critical responder to myocardial inflammation. Through interacting with HSPA8, NLRC5 inhibited the release of IL-6 in macrophages, mitigating cardiomyocyte hypertrophy and cardiac fibroblast activation. More importantly, inhibition of IL-6 by tocilizumab reversed cardiac remodeling and dysfunction in pressure overload-induced models, especially prominently in NLRC5-deficient mice.

TRANSLATIONAL OUTLOOK: Our data suggest that macrophage-derived NLRC5 prevents cardiac inflammation and remodeling, which are recognized pathophysiological mechanisms for the development of HCM and its progression to HF. We also uncovered NLRC5/HSPA8 axis in macrophages as a molecular integrator to facilitate the secretion of IL-6. Blockage of IL-6 by tocilizumab could prevent cardiac remodeling and HF, and the more significant benefit of tocilizumab against cardiac remodeling is achieved when NLRC5 is lacking. Therefore, these data support the possibility of tocilizumab as an alternative immunomodulatory therapeutic strategy for HF.

REFERENCES

1. Heidenreich PA, Bozkurt B, Aguilar D, et al. 2022 AHA/ACC/HFSA guideline for the management of heart failure: a report of the American College of Cardiology/American Heart Association Joint Committee on Clinical Practice Guidelines. *J Am Coll Cardiol*. 2022;79:e263–e421.

2. Nagase T, So YG, Yasui H, et al. Observation of domain wall bimerons in chiral magnets. *Nat Commun*. 2021;12:3490.

3. Ridker PM, Devalaraja M, Baeres FMM, et al. IL-6 inhibition with ziltivekimab in patients at high atherosclerotic risk (RESCUE): a double-blind, randomised, placebo-controlled, phase 2 trial. *Lancet*. 2021;397:2060–2069.

4. Ridker PM, Everett BM, Thuren T, et al. Antiinflammatory therapy with canakinumab for atherosclerotic disease. *N Engl J Med*. 2017;377:1119–1131.

5. Mouton AJ, Li X, Hall ME, Hall JE. Obesity, hypertension, and cardiac dysfunction: novel roles of immunometabolism in macrophage activation and inflammation. *Circ Res*. 2020;126:789–806.

6. Dick SA, Macklin JA, Nejat S, et al. Self-renewing resident cardiac macrophages limit adverse remodeling following myocardial infarction. *Nat Immunol*. 2019;20:29–39.

7. Patel B, Bansal SS, Ismahil MA, et al. CCR2(+) monocyte-derived infiltrating macrophages are required for adverse cardiac remodeling during pressure overload. *J Am Coll Cardiol Basic Trans Science*. 2018;3:230–244.

8. Lim GB. Heart failure: macrophages promote cardiac fibrosis and diastolic dysfunction. *Nat Rev Cardiol*. 2018;15:196–197.

9. Zhao Y, Shao F. NLRC5: a NOD-like receptor protein with many faces in immune regulation. *Cell Res*. 2012;22:1099–1101.

10. Gutte PG, Jurt S, Grutter MG, Zerbe O. Unusual structural features revealed by the solution NMR structure of the NLRC5 caspase recruitment domain. *Biochemistry*. 2014;53:3106–3117.

11. Tong Y, Cui J, Li Q, Zou J, Wang HY, Wang RF. Enhanced TLR-induced NF-kappaB signaling and type I interferon responses in NLRC5 deficient mice. *Cell Res*. 2012;22:822–835.

12. Xu X, Shi Y, Luan P, et al. The subcellular redistribution of NLRC5 promotes angiogenesis via interacting with STAT3 in endothelial cells. *Theranostics*. 2021;11:4483–4501.

13. Luan P, Jian W, Xu X, et al. NLRC5 inhibits neointima formation following vascular injury and directly interacts with PPARgamma. *Nat Commun*. 2019;10:2882.

14. Zhou H, Yu X, Zhou G. NLRC5 silencing ameliorates cardiac fibrosis by inhibiting the TGFbeta1/Smad3 signaling pathway. *Mol Med Rep*. 2017;16:3551–3556.

15. Ma SR, Xie XW. NLRC5 deficiency promotes myocardial damage induced by high fat diet in mice through activating TLR4/NF-kappaB. *Biomed Pharmacother*. 2017;91:755–766.

16. Laroumanie F, Douin-Echinard V, Pozzo J, et al. CD4+ T cells promote the transition from hypertrophy to heart failure during chronic pressure overload. *Circulation*. 2014;129:2111–2124.

17. Tarone G, Brancaccio M. Keep your heart in shape: molecular chaperone networks for treating heart disease. *Cardiovasc Res*. 2014;102:346–361.

18. Willis MS, Patterson C. Hold me tight: role of the heat shock protein family of chaperones in cardiac disease. *Circulation*. 2010;122:1740–1751.

19. Cai WF, Zhang XW, Yan HM, et al. Intracellular or extracellular heat shock protein 70 differentially regulates cardiac remodelling in pressure overload mice. *Cardiovasc Res*. 2010;88:140–149.

20. Cui J, Zhu L, Xia X, et al. NLRC5 negatively regulates the NF-kappaB and type I interferon signaling pathways. *Cell*. 2010;141:483–496.

21. Davis BK, Roberts RA, Huang MT, et al. Cutting edge: NLRC5-dependent activation of the inflammasome. *J Immunol*. 2011;186:1333–1337.

22. Mochizuki D, Adams A, Warner KA, et al. Antitumor effect of inhibition of IL-6 signaling in mucoepidermoid carcinoma. *Oncotarget*. 2015;6:22822–22835.

23. Shinriki S, Jono H, Ota K, et al. Humanized anti-interleukin-6 receptor antibody suppresses tumor angiogenesis and in vivo growth of human oral squamous cell carcinoma. *Clin Cancer Res*. 2009;15:5426–5434.

24. Khanna D, Lin CJF, Furst DE, et al. Tocilizumab in systemic sclerosis: a randomised, double-blind, placebo-controlled, phase 3 trial. *Lancet Respir Med*. 2020;8:963–974.

25. Weissman D, Maack C. Redox signaling in heart failure and therapeutic implications. *Free Radic Biol Med*. 2021;171:345–364.

26. Dridi H, Kushnir A, Zalk R, Yuan Q, Melville Z, Marks AR. Intracellular calcium leak in heart failure and atrial fibrillation: a unifying mechanism and therapeutic target. *Nat Rev Cardiol*. 2020;17:732–747.

27. Adamo L, Rocha-Resende C, Prabhu SD, Mann DL. Reappraising the role of inflammation in heart failure. *Nat Rev Cardiol*. 2020;17:269–285.

28. Gong T, Liu L, Jiang W, Zhou R. DAMP-sensing receptors in sterile inflammation and inflammatory diseases. *Nat Rev Immunol*. 2020;20:95–112.

29. Jaen RI, Val-Blasco A, Prieto P, et al. Innate immune receptors, key actors in cardiovascular diseases. *J Am Coll Cardiol Basic Trans Science*. 2020;5:735–749.

30. Takahashi T, Shishido T, Kinoshita D, et al. Cardiac nuclear high-mobility group box 1 ameliorates pathological cardiac hypertrophy by inhibiting DNA damage response. *J Am Coll Cardiol Basic Trans Science*. 2019;4:234–247.

31. Liu L, Wang Y, Cao ZY, et al. Up-regulated TLR4 in cardiomyocytes exacerbates heart failure after long-term myocardial infarction. *J Cell Mol Med*. 2015;19:2728–2740.

32. Martini E, Kunderfranco P, Peano C, et al. Single-cell sequencing of mouse heart immune infiltrate in pressure overload-driven heart failure reveals extent of immune activation. *Circulation*. 2019;140:2089–2107.

33. Liao X, Shen Y, Zhang R, et al. Distinct roles of resident and nonresident macrophages in nonischemic cardiomyopathy. *Proc Natl Acad Sci U S A*. 2018;115:E4661–E4669.

34. Wang B, Wu Y, Ge Z, Zhang X, Yan Y, Xie Y. NLRC5 deficiency ameliorates cardiac fibrosis in diabetic cardiomyopathy by regulating EndMT through Smad2/3 signaling pathway. *Biochem Biophys Res Commun*. 2020;528:545–553.

35. Shirakawa K, Endo J, Kataoka M, et al. IL (interleukin)-10-STAT3-galectin-3 axis is essential for osteopontin-producing reparative macrophage polarization after myocardial infarction. *Circulation*. 2018;138:2021–2035.

36. Zenke S, Palm MM, Braun J, et al. Quorum regulation via nested antagonistic feedback circuits mediated by the receptors CD28 and CTLA-4 confers robustness to t cell population dynamics. *Immunity*. 2020;52:313–327.e7.

37. Huo S, Shi W, Ma H, et al. Alleviation of inflammation and oxidative stress in pressure overload-induced cardiac remodeling and heart failure via IL-6/STAT3 inhibition by raloxifene. *Oxid Med Cell Longev*. 2021;2021:6699054.

38. Swirski FK, Nahrendorf M. Cardioimmunology: the immune system in cardiac homeostasis and disease. *Nat Rev Immunol*. 2018;18:733–744.

39. Salama C, Han J, Yau L, et al. Tocilizumab in patients hospitalized with covid-19 pneumonia. *N Engl J Med*. 2021;384:20–30.

40. Fajgenbaum DC, June CH. Cytokine storm. *N Engl J Med*. 2020;383:2255–2273.

41. Bijlsma JWJ, Welsing PMJ, Woodworth TG, et al. Early rheumatoid arthritis treated with tocilizumab, methotrexate, or their combination (U-Act-Early): a multicentre, randomised, double-blind, double-dummy, strategy trial. *Lancet*. 2016;388:343–355.

42. Meyer MAS, Wiberg S, Grand J, et al. Treatment effects of interleukin-6 receptor antibodies for modulating the systemic inflammatory response after out-of-hospital cardiac arrest (the IMICA trial): a double-blinded, placebo-controlled, single-center, randomized, clinical trial. *Circulation*. 2021;143:1841–1851.

43. Sun K, Li YY, Jin J. A double-edged sword of immuno-microenvironment in cardiac homeostasis and injury repair. *Signal Transduct Target Ther*. 2021;6:79.

44. Kleveland O, Kunszt G, Bratlie M, et al. Effect of a single dose of the interleukin-6 receptor antagonist tocilizumab on inflammation and troponin T release in patients with non-ST-elevation myocardial infarction: a double-blind, randomized, placebo-controlled phase 2 trial. *Eur Heart J*. 2016;37:2406–2413.

KEY WORDS cardiac remodeling, heart failure, immunomodulatory therapy, macrophages, NOD-like receptor

APPENDIX For an expanded Methods section as well as supplemental figures and tables, please see the online version of this paper.